The Crystal Structure of the Polymerization Catalyst of Acetaldehyde and Its Derivatives. IV. The Crystal and Molecular Structure of Dimethylaluminum *N*-Phenylbenzimidate-*O*-(Trimethylaluminum)-Acetaldehyde Complex, $[(CH_3)_2Al\cdot O\cdot C(C_6H_5){:}N(C_6H_5), CH_3CHO, Al(CH_3)_3]$

Yasushi KAI, Noritake YASUOKA, Nobutami KASAI, and Masao KAKUDO*

Department of Applied Chemistry, Faculty of Engineering, Osaka University, Yamadakami, Suita, Osaka, 565
**Institute for Protein Research, Osaka University, Yamadakami, Suita, Osaka, 565*

(Received May 13, 1972)

The molecular structure of a stereospecific (*isotactic*) polymerization catalyst of the acetaldehyde-monomer-Lewis acid complex, $[Me_2Al\cdot O\cdot CPh{:}\ NPh,MeCHO,AlMe_3]$, has been determined from three-dimensional X-ray-diffraction data collected photographically. The crystal belongs to the monoclinic system (space group $P2_1/n$), with four formula units in a cell with dimensions of: $a=13.60(3)$, $b=13.74(2)$, $c=12.40(2)$ Å, $\beta=95.9(2)°$. The structure was solved by the heavy-atom method and was refined by the block-diagonal, least-squares procedure. The trimethylaluminum forms a bond with the electron-rich oxygen atom of acetaldehyde through the electron-deficient aluminum atom. The polymerization mechanism can reasonably be concluded to be the "co-ordinated cationic polymerization".

During the organochemical investigations of the stereospecific polymerization catalysis of aldehydes, Tani and his co-workers prepared many interesting substances and isolated them in the form of crystals.[1-4] The catalytic system of trialkylaluminum-acid amide gave highly stereospecific polyaldehydes almost quantitatively. The reaction with this catalytic system is mild and has few accompanied side reactions. Therefore, the exact structure determinations of the key substances may reveal much important information about the stereospecific polymerization mechanism. Four compounds were chosen as the key substances in the trimethylaluminum–benzanilide catalyst system; (I) the polymerization catalyst $[Me_2Al\cdot O\cdot CPh{:}\ NPh]_2$, (II) the catalyst-monomer complex $[Me_2Al\cdot O\cdot CPh{:}\ NPh,MeCHO]_2$, (III) the catalyst-monomer-Lewis acid complex $[Me_2Al\cdot O\cdot CPh{:}\ NPh,MeCHO,AlMe_3]$, and (IV) the catalyst-Lewis base complex $[Me_2Al\cdot O\cdot CPh{:}\ NPh,ONMe_3]$. Among these, the molecular structures of I, II, and IV were already reported in detail.[5-7] The complex III, the last one in this series, which is prepared by the equimolar reaction of II and trimethylaluminum in *n*-hexane at 0°C, acts also as the polymerization catalyst of aldehydes, but gives an *atactic* polymer. In this article we will describe the molecular and crystal structure of III. The preliminary results of the structural analysis were communicated earlier.[8] The polymerization mechanism of acetaldehyde has been investigated from the stereochemical point of view on the basis of the molecular structures of these four key substances, together with the organochemical information.

Experimental

The crystals of $[Me_2Al\cdot O\cdot CPh{:}NPh,\ MeCHO,\ AlMe_3]$ were prepared and supplied by Tani snd Yasuda of this University. The compound is very air-sensitive, and the crystal was sealed in a thin-walled glass capillary tube in argon. Two kinds of crystals with different habits were obtained. One of them grows along the *a* axis, and the other, along the *b* axis. Both are colorless, long, and prismatic. The latter crystal examined always had a twinned structure. Figure 1 shows the twinning in the $h0l$ reciprocal lattice plane. The subscript I or II shows to which component each unit cell belongs. The planes containing the $b^*(=b)$ axis and the reciprocal lattice point rows, $h0\bar{h}_I$ and $h0\bar{h}_{II}$, are the twin planes. If the $h0\bar{h}_I$ is taken as c^*_I and the $h0\bar{h}_{II}$ as c^*_{II}, the space group and the twin plane can be described as $P2_1/c$ and the b^*-c^* plane respectively: the same kind of twinning

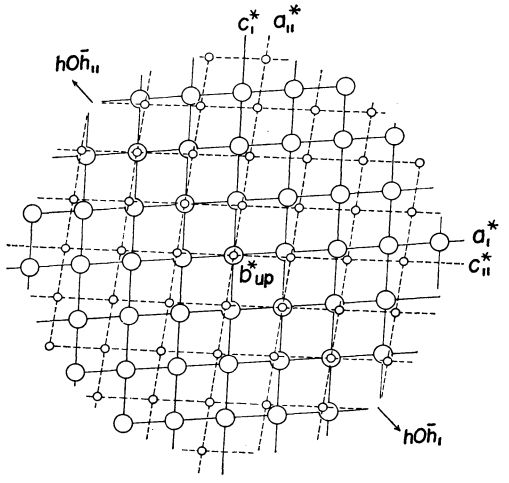

Fig. 1. One reciprocal lattice plane in the twinning crystal of $[Me_2Al\cdot O\cdot CPh{:}\ NPh,MeCHO,AlMe_3]$.

1) H. Tani, T. Araki, and H. Yasuda, *J. Polym. Sci., Part B*, **4**, 727 (1966).
2) H. Tani, T. Araki, and H. Yasuda, *ibid.*, **6**, 389 (1968).
3) H. Tani and H. Yasuda, *ibid.*, **7**, 17 (1969).
4) H. Tani and H. Yasuda, Private Communications.
5) Y. Kai, N. Yasuoka, N. Kasai, and M. Kakudo, *J. Organometal. Chem.*, **32**, 165 (1971).
6) Y. Kai, N. Yasuoka, N. Kasai, and M. Kakudo, This Bulletin, **45**, 3397 (1972).
7) Y. Kai, N. Yasuoka, N. Kasai, and M. Kakudo, This Bulletin, **45**, 3388 (1972).
8) Y. Kai, N. Yasuoka, N. Kasai, M. Kakudo, H. Yasuda, and H. Tani, *Chem. Commun.*, **1970**, 1243.

is found in $[Me_2Al\cdot O\cdot CPh: NPh]_2$.[5] The cell dimensions were determined by a least-squares fitting using the theta values obtained from $0kl$ and $h0l$ Weissenberg photographs. The space group was uniquely determined as $P2_1/n$ from the systematic absence of reflections ($h0l$: $h+l\neq 2n$, and $0k0$: $k\neq 2n$). The crystal data are listed in Table 1. The nickel-filtered Cu$K\alpha$ radiation ($\lambda=1.5418$ Å) was used throughout the X-ray experiments. The crystal density was measured by the flotation method in a mixed solution of carbon tetrachloride and *n*-hexane.

TABLE 1. CRYSTAL DATA OF $[(CH_3)_2Al\cdot O\cdot C(C_6H_5): N(C_6H_5), CH_3CHO, Al(CH_3)_3]$

Monoclinic	$C_{20}H_{29}O_2NAl_2$
$a=13.60(3)$ Å	$M=369.4$
$b=13.74(2)$ Å	$Z=4$
$c=12.40(2)$ Å	$d_m=1.07$ g·cm^{-3}
$\beta=95.9(2)°$	$d_x=1.064$ g·cm^{-3}
$V=2304.8$ Å^3	Space group $P2_1/n$
	$\mu=13.0$cm^{-1}(for Cu$K\alpha$)

The intensity data were collected by multiple-film equi-inclination Weissenberg photographs along the *a* axis only. The intensities were measured visually, and were corrected for the usual Lorentz and polarization factors, as well as for the spot-shape effect. Two independent crystals of a similar size (about $1.0\times0.3\times0.3$ mm) were used. In the layers from $0kl$ through $9kl$, 2891 independent reflections were observed, among which 2336 were non-zero reflections. The interlayer scales were first set proportional to the exposure times and improved in the course of the least-squares refinements with isotropic temperature factors for nonhydrogen atoms.

Structure Determination and Refinement

The structure was established by the heavy-atom method. From a Patterson map, two independent aluminum atoms were easily located. Two successive Fourier maps gave the locations of all the nonhydrogen atoms. The refinement of the structure was done by the method of block-diagonal least-squares. Computations were carried out using the HBLS IV program[9] on a FACOM 230-60 computer at Kyoto University. The function minimized was $\sum w(\Delta F)^2$, and at the intial stage w was taken as unity for all the reflections. The atomic scattering factors used were taken from those of Hanson and his co-workers.[10] Three cycles of the refinement with isotropic temperature factors for nonhydrogen atoms gave the R index of 0.18. Interlayer scales were improved during this refinement and then fixed. Further refinement was followed with anisotropic temperature factors for heavy atoms, and a weighting scheme to be described later was applied. After 2 cycles, the R index was 0.15. At this stage, a difference Fourier synthesis was computed and all the

9) Most of the programs used in the calculations were taken from "The Universal Crystallographic Computing System (I), edited by T. Sakurai, Japanese Crystallographic Association, 1967," and the other programs were cited in our previous paper.[7]

10) H. P. Hanson, F. Herman, J. D. Lea, and S. S. Skillman, *Acta Crystallogr.*, **17**, 1040 (1964).

TABLE 2. ATOMIC CO-ORDINATES OF THE HEAVY ATOMS (IN FRACTION OF CELL EDGES) ALONG WITH THEIR ESTIMATED STANDARD DEVIATIONS (IN 10^{-3} Å)

Atom	x	$\sigma(x)$	y	$\sigma(y)$	z	$\sigma(z)$
Al(1)	0.4154	3	0.2498	2	0.0494	3
Al(2)	0.2925	3	0.1590	3	0.2485	2
O(1)	0.3687	6	0.2321	6	−0.0940	6
O(2)	0.3017	6	0.2015	5	0.1016	5
N	0.2373	6	0.1400	6	−0.0679	6
C(1)	0.4368	13	0.3877	11	0.0736	12
C(2)	0.5242	12	0.1570	14	0.0667	12
C(3)	0.3066	8	0.1688	8	−0.1290	8
C(4)	0.3198	10	0.1273	9	−0.2385	8
C(5)	0.2438	12	0.1143	11	−0.3129	9
C(6)	0.2620	15	0.0815	14	−0.4159	11
C(7)	0.3504	15	0.0589	14	−0.4451	13
C(8)	0.4305	14	0.0656	15	−0.3703	15
C(9)	0.4141	12	0.1034	12	−0.2632	10
C(10)	0.1785	9	0.0521	8	−0.0895	7
C(11)	0.0820	10	0.0563	9	−0.1206	9
C(12)	0.0298	13	−0.0295	12	−0.1405	12
C(13)	0.0809	12	−0.1176	11	−0.1302	12
C(14)	0.1776	11	−0.1219	10	−0.1001	13
C(15)	0.2272	10	−0.0365	9	−0.0777	10
C(16)	0.2168	9	0.1945	8	0.0311	8
C(17)	0.1693	11	0.2934	10	0.0060	10
C(18)	0.1683	14	0.2156	13	0.2981	11
C(19)	0.4141	15	0.2166	15	0.3195	11
C(20)	0.2901	13	0.0167	11	0.2369	11

TABLE 3. ANISOTROPIC TEMPERATURE FACTORS OF THE HEAVY ATOMS EXPRESSED IN THE FORM OF $\exp\{-(\beta_{11}h^2+\beta_{22}k^2+\beta_{33}l^2+\beta_{12}hk+\beta_{13}hl+\beta_{23}kl)\}$

Atom	β_{11}	β_{22}	β_{33}	β_{12}	β_{13}	β_{23}
Al(1)	0.0042	0.0050	0.0071	−0.0020	−0.0013	0.0006
Al(2)	0.0059	0.0061	0.0056	−0.0033	−0.0011	0.0005
O(1)	0.0050	0.0064	0.0076	−0.0035	0.0010	0.0010
O(2)	0.0047	0.0054	0.0053	−0.0006	−0.0012	−0.0004
N	0.0031	0.0049	0.0058	−0.0003	−0.0005	−0.0005
C(1)	0.0116	0.0062	0.0115	−0.0060	−0.0019	0.0002
C(2)	0.0085	0.0120	0.0097	0.0041	0.0042	−0.0019
C(3)	0.0034	0.0053	0.0061	−0.0018	−0.0018	0.0002
C(4)	0.0056	0.0059	0.0064	−0.0015	0.0031	0.0022
C(5)	0.0114	0.0080	0.0049	−0.0041	−0.0006	0.0005
C(6)	0.0150	0.0104	0.0078	−0.0100	−0.0020	−0.0018
C(7)	0.0120	0.0111	0.0125	−0.0064	0.0108	−0.0059
C(8)	0.0084	0.0119	0.0165	0.0016	0.0137	−0.0036
C(9)	0.0086	0.0098	0.0075	−0.0031	0.0048	−0.0023
C(10)	0.0050	0.0050	0.0052	−0.0013	0.0001	−0.0010
C(11)	0.0048	0.0063	0.0085	−0.0008	−0.0017	−0.0005
C(12)	0.0079	0.0096	0.0106	−0.0036	−0.0029	−0.0007
C(13)	0.0080	0.0065	0.0134	−0.0051	0.0021	−0.0031
C(14)	0.0046	0.0068	0.0161	−0.0018	−0.0004	−0.0012
C(15)	0.0065	0.0047	0.0112	0.0030	−0.0031	−0.0016
C(16)	0.0060	0.0052	0.0053	−0.0002	−0.0026	−0.0023
C(17)	0.0089	0.0062	0.0094	0.0052	−0.0041	−0.0030
C(18)	0.0135	0.0099	0.0076	−0.0044	0.0071	−0.0010
C(19)	0.0136	0.0127	0.0069	−0.0104	−0.0054	0.0044
C(20)	0.0117	0.0063	0.0107	−0.0033	−0.0038	0.0044

Table 4. Atomic co-ordinates (in fraction of cell edges) along with their estimated standard deviations (in 10^{-2}Å) and isotropic temperature factors for the hydrogen atoms (in Å^2)

Atom	x	$\sigma(x)$	y	$\sigma(y)$	z	$\sigma(z)$	B
H(1)	0.460	10	0.421	10	0.001	10	3.6
H(2)	0.378	10	0.419	10	0.088	10	3.6
H(3)	0.502	10	0.400	10	0.139	10	3.8
H(4)	0.554	10	0.168	10	0.150	10	3.5
H(5)	0.572	10	0.168	10	0.012	10	3.6
H(6)	0.495	10	0.087	10	0.061	10	3.7
H(7)	0.168	9	0.132	9	−0.294	9	2.3
H(8)	0.197	9	0.076	10	−0.478	10	3.3
H(9)	0.356	11	0.030	11	−0.522	11	4.7
H(10)	0.505	10	0.045	11	−0.389	11	4.3
H(11)	0.484	10	0.115	11	−0.203	10	4.0
H(12)	0.049	12	0.121	13	−0.129	12	5.8
H(13)	−0.050	12	−0.032	12	−0.166	11	5.1
H(14)	0.035	13	−0.178	14	−0.150	13	6.9
H(15)	0.212	10	−0.190	10	−0.094	10	3.3
H(16)	0.303	11	−0.038	11	−0.054	11	4.5
H(17)	0.159	10	0.154	10	0.067	10	3.6
H(18)	0.138	10	0.325	10	0.069	10	3.6
H(19)	0.222	11	0.349	11	−0.007	11	4.2
H(20)	0.142	10	0.290	10	−0.067	10	3.3
H(21)	0.138	9	0.157	10	0.322	9	3.1
H(22)	0.176	11	0.262	10	0.368	11	3.9
H(23)	0.144	10	0.253	11	0.239	11	4.5
H(24)	0.394	11	0.264	11	0.378	11	4.4
H(25)	0.461	10	0.251	9	0.262	10	3.0
H(26)	0.461	10	0.162	10	0.361	10	3.6
H(27)	0.358	10	−0.009	11	0.220	10	4.0
H(28)	0.240	10	−0.010	10	0.180	10	3.6
H(29)	0.272	11	−0.015	11	0.308	11	4.5

hydrogen atoms were located. By including these hydrogen atoms with the isotropic temperature factors, the refinement was done and the R index was reduced to 0.13 after 2 cycles. The difference Fourier map was again computed to obtain improved hydrogen locations. The final refinement gave an R index of 0.124 for non-zero reflections and one of 0.16 for all the reflections. The weighting scheme applied was; $|F_o|<F_{min}$; $w=F_{wt}$, $F_{min}\leqq|F_o|\leqq F_{max}$; $w=1.0$, and $F_{max}<|F_o|$; $w=(F_{max}/|F_o|)^2$, where F_{min}, F_{max}, and F_{wt} were, each changed during the refinements to balance the $\sum w(\Delta F)^2$ over the whole range of $|F_o|$ and $(\sin\theta)/\lambda$. Those values applied at the final refinement were $F_{min}=2.57$, $F_{max}=12.85$, and $F_{wt}=0.15$ respectively.

The final atomic co-ordinates of the heavy atoms, and their estimated standard deviations and the anisotropic temperature factors, are listed in Tables 2 and 3 respectively. The atomic co-ordinates and the isotropic temperature factors of the hydrogen atoms are listed in Table 4. The observed and calculated structure factors are given in Table 5.[11]

11) Table 5 has been submitted to, and is kept as Document No. 7211 by, the office of the Chemical Society of Japan, 1–5 Kanda Surugadai, Chiyoda-ku, Tokyo. A copy may be secured by citing the Document number and by remitting, in advance, ¥ 300 for photo prints. Pay by check or money order payable to: Chemical Society of Japan.

Results and Discussion

Molecular Structure. Figure 2 shows the molecular structure projected along the a axis. The seven atoms of the acetaldehyde moiety are shown as hatched circles. The bond distances and angles were calculated using the DAPH program;[9] they are listed in Tables 6 and 7 respectively.

The trimethylaluminum connects with [$Me_2Al\cdot O\cdot CPh{:}NPh$,MeCHO], one half of the polymerization catalyst-monomer complex, by co-ordination between

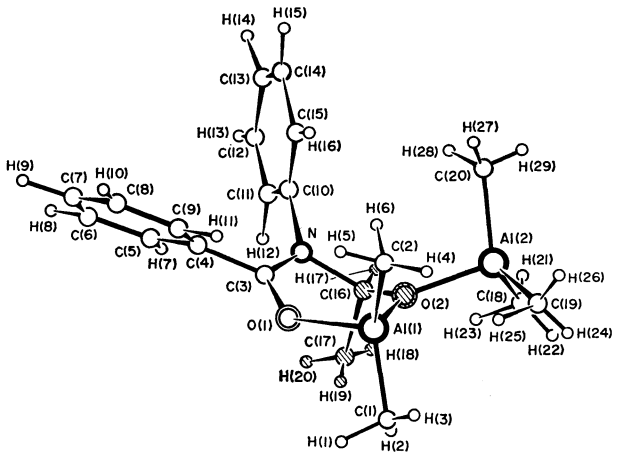

Fig. 2. The molecular structure.

Table 6. Interatomic distances along with their estimated standard deviations

Atoms	Distance (Å)	σ (Å)	Atoms	Distance (Å)	σ (Å)
Al(1)–C(1)	1.936	0.013	Al(2)–C(18)	2.012	0.014
Al(1)–C(2)	1.948	0.014	Al(2)–C(19)	1.960	0.015
Al(1)–O(1)	1.842	0.007	Al(2)–C(20)	1.960	0.013
Al(1)–O(2)	1.860	0.006	Al(2)–O(2)	1.928	0.006
O(1)–C(3)	1.259	0.010	O(2)–C(16)	1.378	0.011
C(3)–N	1.329	0.011	C(16)–C(17)	1.523	0.015
C(3)–C(4)	1.500	0.013	C(16)–N	1.489	0.011
N–C(10)	1.458	0.011	C(16)–H(17)	1.09	0.10
C(4)–C(5)	1.325	0.015	C(10)–C(11)	1.331	0.013
C(5)–C(6)	1.401	0.019	C(11)–C(12)	1.385	0.016
C(6)–C(7)	1.328	0.021	C(12)–C(13)	1.395	0.018
C(7)–C(8)	1.359	0.021	C(13)–C(14)	1.331	0.018
C(8)–C(9)	1.464	0.019	C(14)–C(15)	1.369	0.017
C(9)–C(4)	1.388	0.015	C(15)–C(10)	1.386	0.014
C(1)–H(1)	1.08	0.10	C(18)–H(21)	0.97	0.10
C(1)–H(2)	0.94	0.10	C(18)–H(22)	1.08	0.11
C(1)–H(3)	1.15	0.10	C(18)–H(23)	0.93	0.11
C(2)–H(4)	1.08	0.10	C(19)–H(24)	1.03	0.11
C(2)–H(5)	1.01	0.11	C(19)–H(25)	1.11	0.10
C(2)–H(6)	1.04	0.10	C(19)–H(26)	1.08	0.10
C(17)–H(18)	1.02	0.10	C(20)–H(27)	1.04	0.11
C(17)–H(19)	1.06	0.11	C(20)–H(28)	1.00	0.10
C(17)–H(20)	0.94	0.10	C(20)–H(29)	1.03	0.11
C(5)–H(7)	1.11	0.09	C(11)–H(12)	1.00	0.13
C(6)–H(8)	1.11	0.10	C(12)–H(13)	1.11	0.12
C(7)–H(9)	1.04	0.11	C(13)–H(14)	1.05	0.14
C(8)–H(10)	1.10	0.11	C(14)–H(15)	1.05	0.10
C(9)–H(11)	1.15	0.11	C(15)–H(16)	1.04	0.11

TABLE 7. INTERATOMIC ANGLES ALONG WITH THEIR ESTIMATED STANDARD DEVIATIONS

Atoms	Angle (deg.)	σ (deg.)	Atoms	Angle (deg.)	σ (deg.)
C(1)-Al(1)-C(2)	121.6	0.6	O(2)-Al(2)-C(18)	108.0	0.5
C(1)-Al(1)-O(1)	108.1	0.5	O(2)-Al(2)-C(19)	99.8	0.5
C(1)-Al(1)-O(2)	114.4	0.4	O(2)-Al(2)-C(20)	103.6	0.4
C(2)-Al(1)-O(1)	101.7	0.5	C(18)-Al(2)-C(19)	113.7	0.6
C(2)-Al(1)-O(2)	112.2	0.5	C(18)-Al(2)-C(20)	113.6	0.6
O(1)-Al(1)-O(2)	94.1	0.3	C(19)-Al(2)-C(20)	116.3	0.6
Al(1)-O(1)-C(3)	125.3	0.6	Al(1)-O(2)-Al(2)	125.0	0.3
O(1)-C(3)-N	119.9	0.8	Al(1)-O(2)-C(16)	118.5	0.5
O(1)-C(3)-C(4)	115.9	0.8	Al(2)-O(2)-C(16)	116.6	0.5
N-C(3)-C(4)	124.1	0.7	O(2)-C(16)-N	110.0	0.7
C(3)-N-C(16)	121.7	0.7	O(2)-C(16)-H(17)	111	5
C(3)-N-C(10)	123.3	0.7	O(2)-C(16)-C(17)	112.2	0.8
C(16)-N-C(10)	115.0	0.7	N-C(16)-H(17)	106	5
			C(17)-C(16)-H(17)	104	5
			N-C(16)-C(17)	113.0	0.8
C(3)-C(4)-C(5)	121.6	0.9	N-C(10)-C(11)	121.5	0.8
C(3)-C(4)-C(9)	119.2	0.9	N-C(10)-C(15)	117.4	0.8
C(5)-C(4)-C(9)	119	1	C(11)-C(10)-C(15)	121.1	0.9
C(4)-C(5)-C(6)	119	1	C(10)-C(11)-C(12)	119	1
C(5)-C(6)-C(7)	125	1	C(11)-C(12)-C(13)	119	1
C(6)-C(7)-C(8)	119	1	C(12)-C(13)-C(14)	122	1
C(7)-C(8)-C(9)	117	1	C(13)-C(14)-C(15)	118	1
C(8)-C(9)-C(4)	121	1	C(14)-C(15)-C(10)	121	1
Al(1)-C(1)-H(1)	110	5	Al(2)-C(18)-H(21)	100	6
Al(1)-C(1)-H(2)	111	6	Al(2)-C(18)-H(22)	118	6
Al(1)-C(1)-H(3)	110	5	Al(2)-C(18)-H(23)	102	7
H(1)-C(1)-H(2)	107	8	H(21)-C(18)-H(22)	105	8
H(1)-C(1)-H(3)	105	8	H(21)-C(18)-H(23)	125	9
H(2)-C(1)-H(3)	114	8	H(22)-C(18)-H(23)	108	9
Al(1)-C(2)-H(4)	103	5	Al(2)-C(19)-H(24)	107	6
Al(1)-C(2)-H(5)	112	6	Al(2)-C(19)-H(25)	114	5
Al(1)-C(2)-H(6)	109	6	Al(2)-C(19)-H(26)	111	5
H(4)-C(2)-H(5)	115	8	H(24)-C(19)-H(26)	114	8
H(4)-C(2)-H(6)	107	8	H(24)-C(19)-H(26)	107	8
H(5)-C(2)-H(6)	111	8	H(25)-C(19)-H(26)	105	7
C(16)-C(17)-H(18)	115	6	Al(2)-C(20)-H(27)	110	6
C(16)-C(17)-H(19)	113	6	Al(2)-C(20)-H(28)	115	6
C(16)-C(17)-H(20)	106	6	Al(2)-C(20)-H(29)	111	6
H(18)-C(17)-H(19)	99	8	H(27)-C(20)-H(28)	107	8
H(18)-C(17)-H(20)	126	8	H(27)-C(20)-H(29)	109	9
H(19)-C(17)-H(20)	96	8	H(28)-C(20)-H(29)	104	9
C(4)-C(5)-H(7)	120	5	C(10)-C(11)-H(12)	119	7
C(6)-C(5)-H(7)	121	5	C(12)-C(11)-H(12)	122	7
C(5)-C(6)-H(8)	117	5	C(11)-C(12)-H(13)	124	6
C(7)-C(6)-H(8)	118	5	C(13)-C(12)-H(13)	117	6
C(6)-C(7)-H(9)	119	6	C(12)-C(13)-H(14)	113	8
C(8)-C(7)-H(9)	121	6	C(14)-C(13)-H(14)	125	8
C(7)-C(8)-H(10)	122	6	C(13)-C(14)-H(15)	118	6
C(9)-C(8)-H(10)	121	6	C(15)-C(14)-H(15)	123	6
C(8)-C(9)-H(11)	116	5	C(14)-C(15)-H(16)	120	6
C(4)-C(9)-H(11)	123	5	C(10)-C(15)-H(16)	120	6

the electron-deficient aluminum atom and the electron-rich oxygen atom of the acetaldehyde moiety. In the molecular structure of [dioxane, $(AlMe_3)_2$], a similar co-ordination of $AlMe_3$ to the oxygen atom is found.[12]

12) J. L. Atwood and G. D. Stucky, *J. Amer. Chem. Soc.*, **89**, 5362 (1967).

The Al(2)-O(2) distance of 1.928(6) Å is shorter than the corresponding distance of 2.02(2) Å in [dioxane, $(AlMe_3)_2$]. The geometry of the Al(2) atom is a slightly distorted tetrahedron. The average value of the O(2)-Al(2)-C(methyl) angles of 103.8(0.5)° is a little smaller than that of C(methyl)-Al(2)-C(methyl), 114.5(0.6)°. The average bond distance between Al(2) and three methyl carbons is 1.977(14) Å. The Al(1) atom has a much more distorted tetrahedral geometry than Al(2). The maximum and minimum bond angles around the Al(1) atom are 121.6(0.6)° of C(1)-Al(1)-C(2) and 94.1(0.3)° of O(1)-Al(1)-O(2) respectively.

TABLE 8. THE COMPARISON OF THE SELECTED INTERATOMIC DISTANCES AND ANGLES IN [$Me_2Al\cdot O\cdot CPh{:}NPh$,MeCHO, $AlMe_3$] (III) WITH THE CORRESPONDING VALUES IN [$Me_2Al\cdot O\cdot CPh{:}NPh$, MeCHO]$_2$ (II)

Atoms	(III)	(II)
Al(1)-O(1)	1.842(7) Å	2.045(7) Å
Al(1)-O(2)	1.860(6)	1.858(6)
O(1)-C(3)	1.259(10)	1.265(12)
C(3)-N	1.329(11)	1.364(12)
N-C(16)	1.489(11)	1.469(12)
C(16)-O(2)	1.378(11)	1.418(11)
C(3)-C(4)	1.500(13)	1.455(13)
N-C(10)	1.458(11)	1.466(12)
C(16)-C(17)	1.523(15)	1.559(17)
O(1)-Al(1)-O(2)	94.1(0.3)°	85.1(0.3)°
Al(1)-O(1)-C(3)	125.3(0.6)	127.6(0.6)
O(1)-C(3)-N	119.9(0.8)	119.6(0.8)
C(3)-N-C(16)	121.7(0.7)	120.8(0.7)
N-C(16)-O(2)	110.0(0.7)	110.9(0.7)
C(16)-O(2)-Al(1)	118.5(0.5)	128.0(0.5)

The molecular structure of this compound, except for the trimethylaluminum moiety, is very similar to that of one-half of the polymerization catalyst-monomer complex II. Table 8 compares the selected interatomic bond distances and angles in the present complex, [$Me_2Al\cdot O\cdot CPh: NPh$,MeCHO,$AlMe_3$] (III), with those of the corresponding parts in [$Me_2Al\cdot O\cdot CPh: NPh$,MeCHO]$_2$ (II). In Fig. 3 are compared the molecular structures of II and III projected onto the O-C-N plane of the amide moiety, which is present in both complexes. The numbers in brackets show the deviations of each atom from the O-C-N plane (in Å units).

The Al(1)-O(1) distance in II is much longer than that in III. This may be due to the difference in the co-ordination geometries of aluminum atoms. In the complex II the aluminum atom is penta-co-ordinated, it has a trigonal-bipyramidal geometry, and the oxygen atom of the amide moiety, O(1), occupies the apical position. The Al(1)-O(2) bond distances, on the contrary, show a good agreement in these two compounds. The C-O bond distance in the co-ordinated aldehyde moiety in III, C(16)-O(2)=1.378(11) Å, is a little shorter than the normal C-O single bond distance, though not significantly so. The C(16)-C(17) (1.523 (15) Å) and N-C(16) (1.489(11) Å) distances agree well with the respective expected single-bond distances.

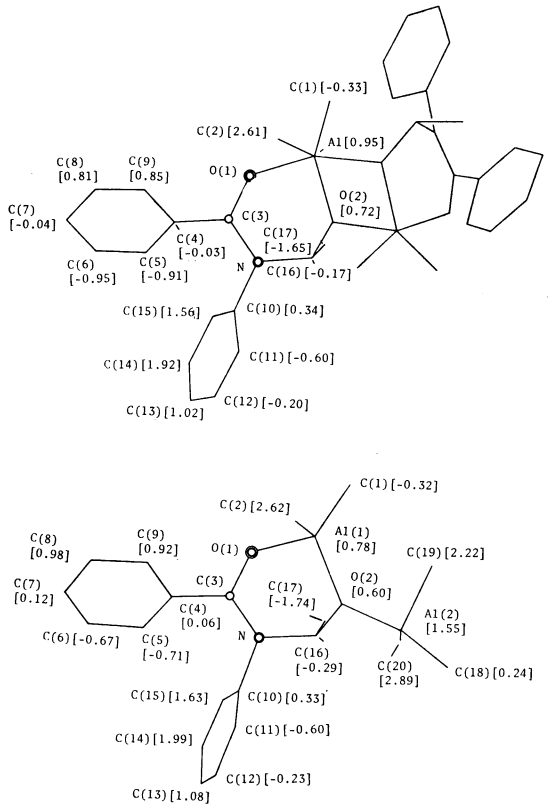

Fig. 3. Comparison of the molecular structure of [$Me_2Al\cdot O\cdot CPh{:}NPh$,MeCHO]$_2$ (*top*) and [$Me_2Al\cdot O\cdot CPh{:}NPh$, MeCHO,$AlMe_3$] (*bottom*). Both are projected onto the plane of the –O–C–N– skeletons which are contained commonly in both molecules. Deviations from the plane (in Å) are given in brackets.

The two adjacent benzene rings in the amide moiety in III have a *cis* configuration, and the internal rotation angle around the C(3)–N bond is 12.7°. The dihedral angle between the best planes of these rings is 67.4°.

Crystal Structure. Figure 4 shows the molecular packing in the unit cell. The intermolecular atomic contacts shorter than 3.8 Å are shown by the broken lines. These are the usual van der Waals' contact distances.

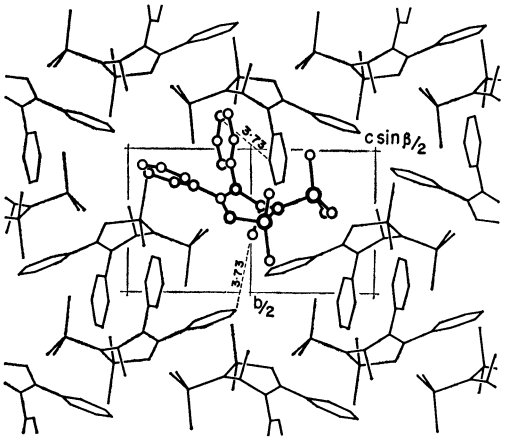

Fig. 4. Crystal structure viewed along the *a* axis.

Polymerization Mechanism in This Catalytic System

In the catalytic system of the highly stereospecific polymerization of acetaldehyde, we have previously undertaken the X-ray structure analysis of the following four key substances in an attempt to clarify the reaction mechanism. They are;

(I) [$Me_2Al\cdot O\cdot CPh{:}NPh]_2$

(II) [$Me_2Al\cdot O\cdot CPh{:}NPh$, $MeCHO]_2$

(III) [$Me_2Al\cdot O\cdot CPh{:}NPh$, MeCHO, $AlMe_3$]

(IV) [$Me_2Al\cdot O\cdot CPh{:}NPh$, $ONMe_3$]

The molecular geometries of these four complexes and the organochemical backgrounds have already been reported.[1–8] Figure 5 shows the molecular structures of these complexes viewed along arbitrary orientations, for an easy understanding of them (the numbers from I to IV correspond to the above complexes).

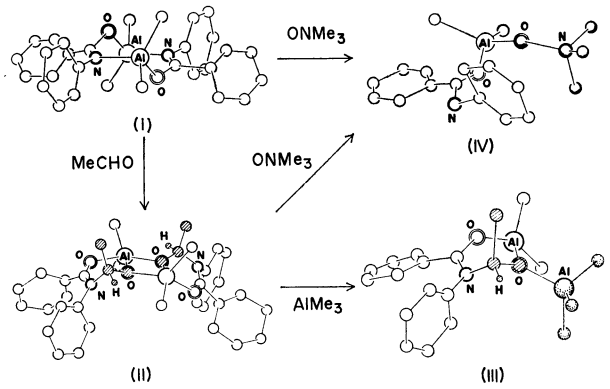

Fig. 5. Moleculer structures and their reactions of four key substances in the catalytic system of trimethylaluminum-benzanilide.

The dimeric catalyst I takes an imino-ether-type structure: a centro-symmetrical eight-membered ring is composed of the –O–C–N– bridges of amide moieties between two aluminum atoms. The complex IV is monomeric and *catalytically inactive.* The Al–O–C–N moiety takes the same configuration as the monomeric unit of the catalyst I, except that two benzene rings adopt a *trans* configuration.

The catalyst-monomer complex II has a dimeric structure related by the two-fold axis. The aldehyde moiety is maintained by the catalyst at the sites of both oxygen and α-carbon atoms. The oxygen atom co-ordinates to the two aluminum atoms, and the α-carbon atom bonds to the nitrogen of the amide moiety. However, the Al–O–C–N moiety takes a different configuration from that in I or IV. In the structure of III, the configuration of the monomeric unit of II is exactly maintained. The typical Lewis acid, $AlMe_3$, attacks and co-ordinates to the aldehyde oxygen atom, but not to the amide oxygen. This suggests that the aldehyde oxygen atom is more active than the amide oxygen in response to the attack of the electrophilic reagent.

Besides the above-mentioned molecular geometries, much chemical evidence has been accumulated.[1–4]

They are: (a) both catalysts, I and II, lose their activities when they are absolutely dried; a small amount of water behaves as the co-catalyst in this system, and both the yield of polymer and the stereospecificity of the polymerization reach their maxima at the optimum water concentration (1/30 mole per mole of the catalyst I, *i.e.*, *ca.* 1×10^{-4} mol% of the aldehyde); and (b) the polymerization is hindered by the existence of the strong electron donor. These two facts show that the polymerization system belongs to the cationic type; we will call the present polymerization the "co-ordinated cationic polymerization". Other important evidences are: (c) the aldehyde moiety of II can be easily replaced by a free aldehyde present in the solution; and (d) the water which is a co-catalyst in this system does not affect the exchange reaction of aldehyde.

In the reaction from I to II, we can postulate the following steps: (1) the fission of the Al–N bond in I induced by the co-ordination of the acetaldehyde to the aluminum atom by its oxygen, as in the co-ordination of $ONMe_3$ in IV; (2) the formation of an imino-ether-type intermediate, in which two benzene rings take a stable *trans* configuration; (3) bond formation between the nitrogen atom (in amide) and α-carbon (in aldehyde), followed by the configurational change of benzene rings from *trans* to *cis*, and (4) dimeric association. The association reaction is placed last because the cryoscopic measurement of the molecular weight of II shows the compound is likely to be monomeric in such a dilute solution as in the present polymerization conditions; this may be supposed on the basis of the long Al–O (aldehyde oxygen) distance of 1.985(6) Å. The formation of the monomeric complex III also supports the dissociation of the II in the dilute solution. The configurational change from (1) to (4) was examined by using a molecular model reported elsewhere.[7]

From the knowledge of the molecular structures given by the chemical evidence, a plausible mechanism of *isotactic* polymerization is proposed; it is shown in Fig. 6 (Schemes V to VII).

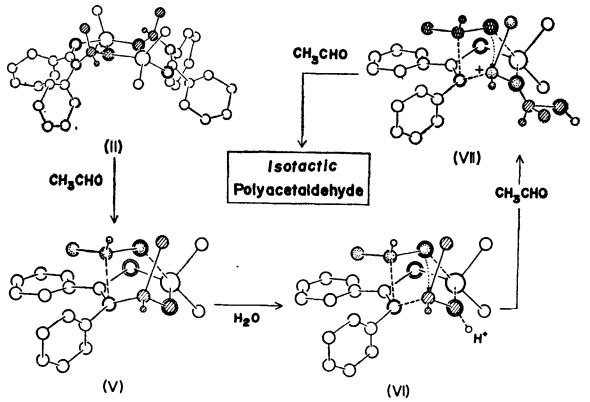

Fig. 6. Proposed mechanism for stereospecific polymerization of acetaldehyde.

The scheme V is constructed as an intermediate complex both for the aldehyde exchange reaction and for the initiation of the polymerization reaction. The broken lines show the postulated weak bonds caused by the co-ordination of the aldehyde. Model examination shows that the steric hindrance gives little possibility of taking a co-ordination other than that drawn in the scheme V. This fact probably contributes to the stereospecificity of the polymerization. In the exchange reaction, the aldehyde moiety in the catalyst is replaced by the weakly co-ordinated second aldehyde and there is no further change.

In the polymerization initiation, the formation of a chemical bond takes place between these two aldehyde molecules. This case is shown in scheme VI. First, a proton (probably from the water, the co-catalyst) attacks the oxygen atom of the initially-co-ordinated aldehyde, as the trimethylaluminum attacks the corresponding aldehyde oxygen in II. Then the cationic character of the proton transfers to the oxygen to form an oxonium cation, which weakens the co-ordination bond between the oxygen and aluminum atoms. After that, the cationic character moves to the α-carbon atom and generates a carbonium cation, which increases the affinity to the oxygen atom of the secondary co-ordinated aldehyde and at the same time weakens the bonding to the nitrogen atom. The secondary co-ordinated aldehyde now adds to the initially-co-ordinated one, and the aldehyde dimer thus formed replaces the initially co-ordinated aldehyde. The replacement is accompanied by the stimulation of the co-ordination of a new, third aldehyde. This is shown in scheme VII. The new aldehyde adds to the dimer, and the newly-formed trimer replaces the dimer in its co-ordination. The succession of these reactions produces the linear *isotactic* polymer of acetaldehyde.

As has been reported, the polymerization of acetaldehyde by the catalysis of complex III gives an *atactic* polymer. This fact can be explained by the dissociation of trimethylaluminum from III. The trimethylaluminum itself also acts as a polymerization catalyst and gives an *atactic* polyaldehyde under the conditions of the polymerization reaction by the complex III.[4] The polymerization reaction by the I or II catalyst is very mild compared with the reaction by the trimethylaluminum itself. Therefore, if the complex III is placed under the polymerization conditions, the dissociation of trimethylaluminum from this complex occurs. The dissociated trimethylaluminum acts predominantly as a polymerization catalyst and gives an *atactic* polymer.

The authors wish to express their deep thanks to Professor Hisaya Tani and Dr. Hajime Yasuda of Osaka University for their kindness in supplying the samples and for many their helpful discussion.